

# Dependence of cluster ion emission from uranium oxide surfaces on the charge state of the incident slow highly charged ion

A. V. Hamza<sup>a</sup>, T. Schenkel, and A. V. Barnes

University of California, Lawrence Livermore National Laboratory, Livermore, CA 94551, USA

Received: 24 August 1998 / Received in final form: 20 November 1998

**Abstract.** The cluster ion yields and cluster ion distribution for highly charged ion sputtering have been measured for a uranium oxide target for Xe<sup>44+</sup>, Au<sup>63,66,69+</sup> and Th<sup>75+</sup> incident ions. The cluster yields exhibit a power law dependence on the cluster size with exponents increasing from  $-4$  to  $-2.4$  with increasing primary ion charge from 44+ to 75+. The power law exponent is also correlated with the total sputter yield.

**PACS.** 36.40.-c Atomic and molecular clusters – 61.46.+w Clusters, nanoparticles, and nanocrystalline materials – 82.65.-i Surface and interface chemistry

## 1 Introduction

Cluster emission phenomena are of scientific and technological interest because of the potential for clusters to form materials with new chemical and physical properties. In addition, studies of the cluster yields due to surface excitation will lead and have led to a better understanding of the excitation mechanism and sputtering process.

The most easily accessible experimental information on the cluster formation process is the cluster partial yield or the cluster size distribution. Two methods of obtaining this distribution have been used extensively: measurement of the charged cluster distribution and post-ionization of the neutral clusters with either electrons or photons beams. The first method suffers from the fact that the probability of cluster ionization increases with cluster size [1, 2]. The second method suffers from the unknown fragmentation probability of the clusters in the post-ionization step [1, 3]. In the case of metal clusters, a rather large difference in the cluster distribution has been reported depending on the method used [2]. In the case of non-metallic clusters, the ionization probability is relatively constant with cluster size, particularly if the  $n = 1$  cluster is not considered. The ionization potential for van der Waals, Ar<sub>*n*</sub> and Kr<sub>*n*</sub> clusters is independent of cluster size,  $n$ , from 2 to 24 [4]. Even for metal atoms, small clusters may not exhibit metallic properties. One example of this is Hg<sub>*n*</sub> clusters, where for  $3 < n < 13$  the ionization potential is approximately constant; this effect is ascribed to non-metallic behavior of these mercury clusters [5]. Wucher *et al.* [2] have shown *via* comparison of neutral metal cluster yields measured by laser post-ionization and ionized metal

cluster yields that the ionization probability for clusters greater than  $n = 5$  is fairly constant, though oscillation of ion stabilities are observed.

Measurements of cluster ion yields at short times (much less than 1  $\mu$ s) do not exhibit oscillations [6]. Mass spectra at late times (greater than 1  $\mu$ s) are influenced by relative cluster ion stabilities [6]. In the measurements presented here, the cluster ions are detected in the intermediate time regime of  $\sim 0.1$ -1  $\mu$ s. If the clusters break up after acceleration they will not significantly degrade the arrival time over that caused by the initial velocity spread. The stops generated by the fragments will have very close to the correct time of arrival for the parent cluster. We do not observe any effects due to ion stabilities for uranium oxide clusters (see below). Since ion production occurs at short times, cluster ion stability is unimportant in the ion production process. Thus, the distribution of ionized non-metallic clusters for cluster size  $n > 1$  gives a relatively faithful picture of the relative neutral cluster distribution. We, therefore, report the ionized uranium oxide cluster yield as representative of the neutral cluster uranium oxide yield.

From the results presented below and previous work [1, 7–9] it is observed that a power law cluster yield distribution according to

$$Y(n) \propto n^{-\tau} \quad (1)$$

is a general phenomenon. The observed value of  $-\tau$  varies between  $-2$  and  $-15$  depending upon sputtering conditions such as the incident kinetic energy, projectile charge, and angle of incidence of the projectile and on the material properties of the target surface. Wucher and co-workers [2, 7, 10] have proposed and demonstrated for the case of

<sup>a</sup> e-mail: Hamza1@llnl.gov

silver clusters that the value of  $-\tau$  is correlated to the total sputtering yield of the sample in such a way that when the total sputter yield increases the value of  $-\tau$  increases. This correlation is also supported by measurements on copper [1].

Only two published models predict a power law cluster yield distribution. The first is a shock wave initiated process of Parilis and Bitensky [11]. The assumption is that momentum is transferred to near-surface target molecules due to the propagation of a pressure pulse or shock wave, resulting in the emission of large clusters. The predicted exponent for the power law is  $-\tau \sim -2$ . However, the exponent,  $-\tau$ , is fixed by the physics of the model and can not explain the variation with total sputter yield.

The second model that predicts a power law cluster yield distribution is the model by Urbassek [3] which is applicable to sputtering by both singly and highly charged ions. In this “equilibrium” model, a highly energized region of the surface undergoes a liquid-gas phase transition upon expanding into vacuum. If the phase transition happens near the critical point (where interparticle binding is just balanced by the kinetic energy), fluctuations are high enough to produce high yields of large clusters. In this model the clusters are assumed to be in equilibrium with each other and monoatomic species. The cluster yield depends on the energy deposited into the near-surface volume. Reaching the critical point requires the kinetic energy of the target atoms be high, so that chemical bonding loses its importance and the system becomes fluid. Slow, highly charged ions can liberate a large amount of their potential energy (100–300 keV per ion) into a small nanometer sized volume on very short, femtosecond, time scales [12, 13]. The equilibrium model predicts transitions from an exponential decay to power law decay as the phase transition occurs closer to the critical point. The dependence of the cluster yield  $Y(n)$  on the cluster size,  $n$ , is

$$Y(n) = Y_0 n^{-\tau} \exp\left[\frac{-\Delta G n - 4\pi n^{2/3} r^2 \sigma}{kT}\right], \quad (2)$$

where  $\Delta G$  is the difference of the Gibbs free energies of the liquid and gas phase,  $k$  is Boltzmann’s constant,  $T$  is the temperature of the energized region,  $Y_0$  is the sputter yield,  $r$  is the cluster radius,  $\sigma$  is the surface tension and  $-\tau$  is the critical exponent. At equilibrium  $\Delta G$  is zero and at the critical point the surface tension vanishes. Thus, the power law exponent at the critical point is  $-\tau$ , with  $-\tau$  between  $-2$  and  $-2.5$ . It follows that predicted cluster size distributions at the critical point are very similar for the equilibrium and shock wave models. The equilibrium model can explain changes in the power law exponent over a narrow range. Should the energy deposition be insufficient to reach the critical point, the surface tension term will introduce deviations from the  $-\tau$  equal to  $-2$  description. Unfortunately, observed power law exponents of less than  $-5$  cannot be explained because of the dominance of the exponential term for larger  $n$ .

Neither model, shock wave or equilibrium, has any explicit dependence of the power law exponent on the total sputter yield.

In this paper the emission of clusters from uranium oxide surfaces upon impact of highly charged ions will be presented. The cluster ion yield *versus* cluster size will be discussed in the context of the above models and presented as a function of the total sputter yield. The total sputter yields for highly charged ion sputtering from uranium oxide surfaces have been presented previously [14].

## 2 Experimental

Highly charged ions were extracted from the electron beam ion trap (EBIT) at Lawrence Livermore National Laboratory [15]. A bending magnet in the beamline between the EBIT and the UHV scattering chamber (base pressure  $< 3 \times 10^{-8}$  Pa) is used to select the mass-to-charge ratio of the incident ion beam. Time-of-flight secondary ion mass spectrometry (TOF-SIMS) was performed to measure cluster yields. The system is described in references [16] and [17]. Briefly, fluxes of  $< 1000$  ions per second were used and each TOF-SIMS cycle was triggered by secondary particles emitted from the target on impact of an individual HCI at normal incidence. High yields of electrons and protons were used as start pulses for the time of flight for negative and positive secondary ions, respectively. Start efficiencies were 100% for electron starts and between 10 and 80% for proton starts. Start signals and secondary ion stop signals were detected by the same annular microchannel plate detector. The microchannel plate detection efficiency for secondary ions is estimated from the solid angle subtended and the active area to be  $\sim 10$  to 15%. TOF-SIMS spectra are recorded with a multi-stop multichannel scaler.

Polycrystalline uranium ( $^{238}\text{U}$ ) targets were prepared by electropolishing followed by oxidation in air for several hours for native oxide formation. The oxide thickness was estimated from known oxidation rates [18] to be several hundred nanometers. Targets were cleaned after insertion into vacuum by low energy ion sputtering. The pressure in the target chamber was kept below  $5 \times 10^{-10}$  Torr. Surface conditions were monitored closely by TOF-SIMS. Secondary ion spectra were reproducible over several sputter cleaning cycles.

## 3 Results and discussion

The cluster ion yields and cluster ion size distribution for highly charged ion sputtering have been measured for a uranium oxide target for  $\text{Xe}^{44+}$ ,  $\text{Au}^{63,66,69+}$  and  $\text{Th}^{75+}$  incident ions. A representative secondary ion mass spectrum for  $\text{Au}^{69+}$  impinging on  $^{238}\text{UO}_2$  with 220 keV kinetic energy is shown in Figure 1. Uranium oxide clusters  $(\text{UO}_x)_n^+$  are observed to  $n = 7$  in this example. A plot of the cluster yield (secondary cluster ions per primary ion) as a function of cluster size ( $n$ ) is shown in Figure 2 for  $\text{Th}^{75+}$  primary ions. As can be observed in Figure 1 secondary ions with varying oxygen content are observed. The effect of the oxygen content on the cluster ionization probability

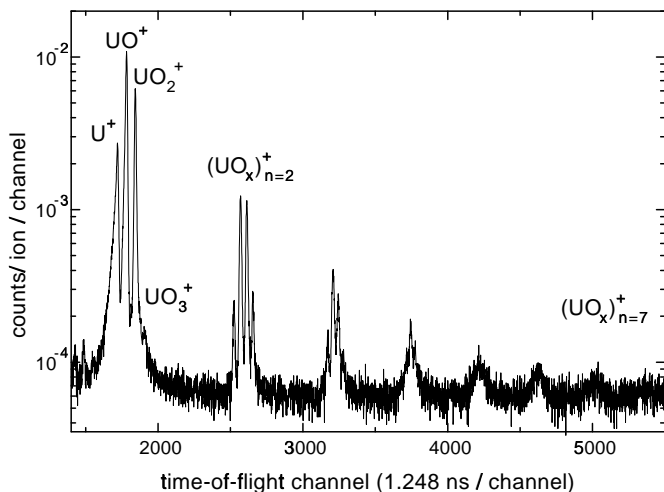


**Fig. 1.** Highly charged ion based secondary ion mass spectrum from  $\text{Au}^{69+}$  impinging on  $^{238}\text{UO}_2$  [14].

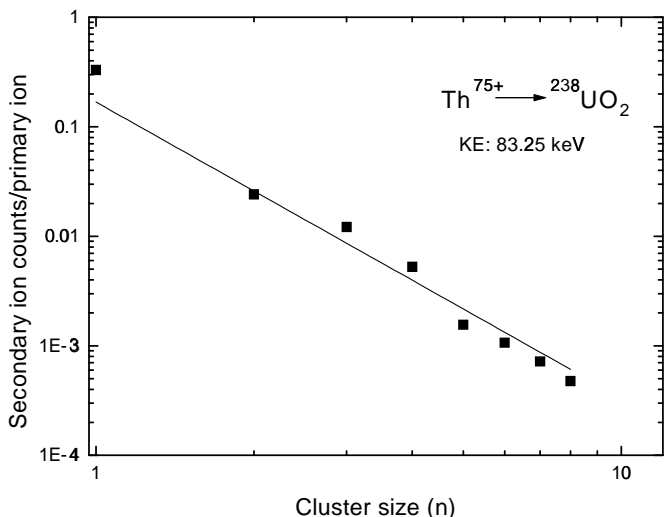


**Fig. 2.** Plot of secondary cluster ion counts per incident  $\text{Th}^{75+}$  ion versus cluster size ( $n$ ). The solid line is a power law fit to the data with exponent  $-2.7 \pm 0.2$ .

is unknown. For the analysis presented here all the various  $(\text{UO}_x)_n^+$  clusters were added together for a given  $n$  to determine the partial ion yields. The cluster partial yield exhibited a power law dependence on the cluster size with an exponent of  $-2.7 \pm 0.2$ . The cluster partial yields exhibited a power law dependence on the cluster size with exponents increasing from  $-4$  to  $-2.4$  with increasing primary ion charge from  $44+$  to  $75+$ . Since the total sputter yield increases as the charge of the incident ion increases, it is instructive to plot the power law exponent versus total sputter yield.

The power law exponent varies with the total sputter yield. Figure 3 shows the dependence of the power law exponent on the total sputter yield for slow, highly charged ions impinging on  $^{238}\text{UO}_2$  with kinetic energies between  $80$  and  $500$  keV. The total sputter yields as a function of incident charge state were measured under identical sur-

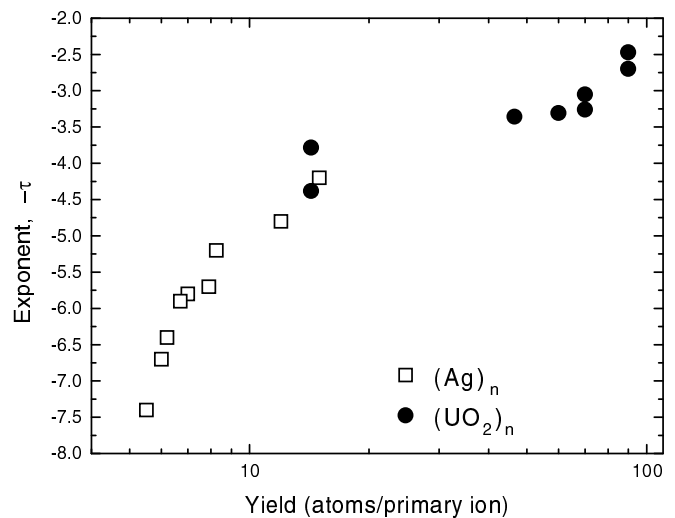


**Fig. 3.** Plot of power law exponent versus total sputter yield for slow, highly charged ions impinging on  $^{238}\text{UO}_2$  (present work) and  $\text{Ar}^+$  ions impinging on  $\text{Ag}$  surfaces [7].

face conditions by the “catcher foil” technique at  $0.3v_{\text{bohr}}$  for the incident primary ion as reported by Schenkel *et al.* [14]. Since the catcher foil experiments only determine the number of uranium atoms removed per incident primary ion, the uranium atom removal is used as the total sputter yield plotted in Figure 3. The sputter yields were determined at, in some cases, different kinetic energies than the partial cluster ion yields. As shown previously the kinetic energy of the Xe projectiles have no measurable effect on the ion yields [14] and, by extension, on the total yields. The kinetic energy of the Th and Au projectiles have at most a 23% effect on the ion yield [14] and hence, by extension, the total sputter yield. In addition the total sputter yield was measured only up to charge state  $70+$  ( $\text{Th}^{70+}$ ). Thus, the total sputter yield for charge state  $75+$  ( $\text{Th}^{75+}$ ) is an extrapolation of the data in reference [14].

As the total sputter yield increases the exponent increases, approaching the  $-2$  limit of both the shock wave model and the equilibrium model. Also shown is the dependence of the power law exponent on total sputter yield for singly charged  $\text{Ar}^+$  ions impinging on  $\text{Ag}$  surfaces [7]. It should be stressed that the silver partial cluster yields were measured by photoionization of the neutral clusters and the reported  $\text{UO}_2$  partial cluster yield is the cluster ion yield. We believe it is fortuitous that for similar total sputter yields for  $\text{UO}_2$  and  $\text{Ag}$ , the power law exponent is the same. However, the trend is quite compelling that increased sputter yields give increased power law exponents. While it is tempting to ascribe the observation of power law behavior with critical point exponents to achieving critical point conditions, this cannot unambiguously be claimed. However, if a critical point were reached the power law with critical exponent would be observed. These data suggest that as the deposited energy density increases, as occurs with increasing the charge state of the incident ion, critical behavior may be approached.

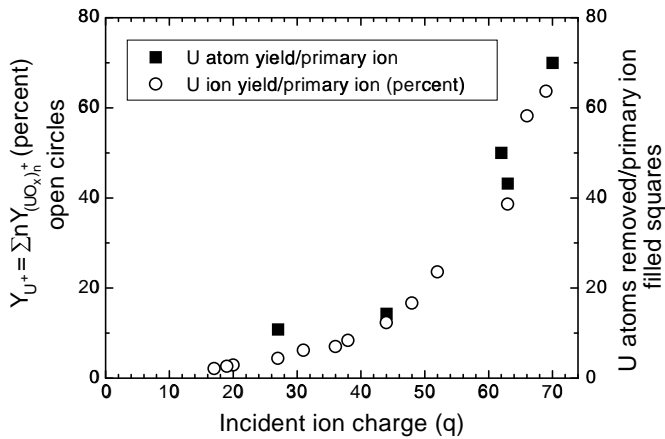


**Fig. 4.** Plot of total uranium emitted as cluster ions *versus* incident ion charge (open circles) and the total sputter yield of uranium (atoms removed per incident ion) *versus* incident ion charge (filled squares).

The relationship of the power law exponent,  $-\tau$ , with total number of uranium atoms emitted as cluster ions from the solid would be very similar to the relationship of the power law exponent with the total number of uranium atoms ejected shown in Figure 3. Figure 4 shows a comparison of the dependence of the total number of uranium atoms emitted as cluster ions on the incident charge state of the highly charged ion to the dependence of the total sputter yield (U atoms ejected per primary ion) on the incident charge state of the highly charged ion. The total U emitted as cluster ions is defined by

$$Y_{U^+} = \sum n Y_{(UO_x^+)_n},$$

where  $Y_{(UO_x^+)_n}$  is the secondary ion yield of  $(UO_x^+)_n$ . For charged states greater than 40+, where the partial cluster yields become appreciable, the total U emitted as cluster ions is proportional to the total U atom removal or total sputter yield.

Recent measurements by Hansen *et al.* [19] have shown a deviation from the dependence of the power law exponent with total sputter yield (see above). In this case calcium cluster sputtering was shown to follow the power law behavior; however, the power law exponent was lower (by about a factor of 2) than would be expected for the total sputter yield compared with other metal clusters. This anomaly was ascribed to the low energy of formation for small Ca clusters as evidenced by the very weak dimer bond (0.14 eV [20]). The very high cohesive energy of uranium oxide (22 eV [21]) and uranium (5.5 eV [22]) suggests the energy of formation of  $UO_2$  clusters is sufficient to observe the “normal” power law *versus* sputter yield dependence, which is the case. The previous measurements of Schenkel *et al.* [9] showed that the power law cluster distributions are observed for non-homonuclear surfaces and for highly charged ion sputtering. The measurements reported here show the power law exponent dependence with total sputter yield holds for non-homonuclear, non-metallic surfaces and highly charged ion sputtering as well.

A number of recent molecular dynamics simulations of the sputtering of metal surfaces by singly charged ions have been performed for copper [23,24], silver [10,25], and indium-gallium [26]. These simulations have been able to reproduce the power law dependence of the partial cluster yield and the dependence of the power law exponent on the total sputter yield. The main conclusion is that the cluster emission process involves a correlated emission (“emission as entity”). Also important in the simulations to predict the correct power law exponents is a correct binding of the cluster atoms. If the cluster binding energy is too high the power law exponent is over estimated. Unfortunately, the simulations do not provide a simple physical picture of the origin of the power law behavior or the dependence on the total sputter yield.

## 4 Summary

The partial cluster yield of  $(UO_x^+)_n$  clusters from  $UO_2$  surfaces follows a power law decay upon highly charged ion excitation. The power law exponent increases with increasing charge of the incident primary ion. At the highest charge states for the primary ion, the power law exponent approaches the  $-2$  limit of both the shock wave model and the equilibrium model. The experimental finding that the power law exponent which describes cluster sputtering increases with increasing total sputter yield is extended to higher sputter yields ( $> 50$  sputtered uranium atoms per incident primary ion). Also demonstrated is that this experimental finding is equally applicable to singly charged and highly charged ion sputtering. The dependence of the power law exponent on total sputter yield is also extended to non-homonuclear and non-metallic solid surfaces.

This work was performed under the auspices of the U. S. Department of Energy at Lawrence Livermore National Laboratory under contract number W-7405-ENG-48.

## References

1. S.R. Coon, W.F. Calaway, M.J. Pellin, J.M. White, *Surf. Sci.* **298**, 161 (1993).
2. A. Wucher, M. Wahl, H. Oechsner, *Nucl. Inst. Meth. Phys. Res. B* **83**, 73 (1993).
3. H.M. Urbassek, *Rad. Eff. Defects Solids* **109**, 293 (1989); H.M. Urbassek, *Nucl. Inst. Meth. Phys. Res. B* **31**, 541 (1988).
4. W. Kamke, J. de Vries, J. Krauss, E. Kaiser, B. Kamke, I.V. Hertel, *Z. Phys. D* **14**, 339 (1989).
5. K. Rademann, B. Kaiser, U. Even, F. Hensel, *Phys. Rev. Lett.* **59**, 2319 (1987).
6. W. Ens, R. Beavis, K.G. Standing, *Phys. Rev. Lett.* **50**, 27 (1983).
7. A. Wucher, M. Wahl, *Nucl. Inst. Meth. Phys. Res. B* **115**, 581 (1996).
8. Z. Ma, S.R. Coon, W.F. Calaway, M.J. Pellin, D.M. Gruen, E.I. von Nagy-Felsobuki, *J. Vacuum Sci. Technol. A* **12**, 2425 (1994).

9. T. Schenkel, A.V. Barnes, A.V. Hamza, D.H. Schneider, *Eur. Phys. J. D* **1**, 297 (1998).
10. A. Wucher, *Nucl. Inst. Meth. Phys. Res. B* **83**, 79 (1993).
11. I.S. Bitensky, E.S. Parilis, *Nucl. Inst. Meth. B* **21**, 26 (1987).
12. T. Schenkel, M.A. Briere, A.V. Barnes, A. Hamza, K. Bethge, H. Schmidt-Böcking, D.H. Schneider, *Phys. Rev. Lett.* **79**, 2030 (1997).
13. T. Schenkel, M.A. Briere, H. Schmidt-Böcking, K. Bethge, D.H. Schneider, *Phys. Rev. Lett.* **78**, 2481 (1997).
14. T. Schenkel, A.V. Barnes, A.V. Hamza, D.H. Schneider, J.C. Banks, B.L. Doyle, *Phys. Rev. Lett.* **80**, 4325 (1998).
15. D. Schneider, M.W. Clark, B.M. Penetrante, J. McDonald, D. DeWitt, J.N. Bardsley, *Phys. Rev. A* **44**, 3119 (1991).
16. D. Schneider, M.A. Briere, *Phys. Scripta* **35**, 228 (1996).
17. T. Schenkel, A.V. Barnes, M.A. Briere, A. Hamza, A. Schach von Wittenau, D.H. Schneider, *Nucl. Inst. Meth. Phys. Res. B* **125**, 153 (1997).
18. G.W. McGillivray, D.A. Geeson, R.C. Greenwood, *J. Nucl. Mat.* **208**, 81 (1994).
19. C.S. Hansen, W.F. Calaway, B.V. King, M.J. Pellin, *Surf. Sci.* **398**, 211 (1998).
20. C.R. Vidal, *J. Chem Phys.* **72**, 1864 (1980).
21. T. Petit, B. Morel, C. Lemaignan, A. Pasturel, B. Bigot, *Phil. Mag. B* **73**, 893 (1996).
22. C. Kittel, *Introduction to Solid State Physics*, fifth edition (John Wiley & Sons, New York, 1976).
23. G. Betz, W. Husinsky, *Nucl. Inst. Meth. Phys. Res. B* **102**, 281 (1995).
24. M.H. Shapiro, T.A. Tombrello, *Radiat. Eff. Defects Solids* **130**, 235 (1994).
25. A. Wucher, B.J. Garrison, *J. Chem. Phys.* **105**, 5999 (1996).
26. J.W. Hartman, M.H. Shapiro, T.A. Tombrello, *Nucl. Inst. Meth. Phys. Res. B* **124**, 31 (1997).